Effects of nonlocal feedback on traveling fronts in neural fields subject to transmission delay

A. Hutt*
Weierstrass-Institute for Applied Analysis and Stochastics, Mohrenstrasse 39, 10117 Berlin, Germany
(Received 28 May 2004; published 11 November 2004)

The work introduces a model for reciprocal connections in neural fields by a nonlocal feedback mechanism, while the neural field exhibits nonlocal interactions and intra-areal transmission delays. We study the speed of traveling fronts with respect to the transmission delay, the spatial feedback range, and the feedback delay for general axonal and feedback connectivity kernels. In addition, we find a novel shape of traveling fronts due to the applied feedback and criteria for its occurrence are derived.

DOI: 10.1103/PhysRevE.70.052902 PACS number(s): 87.19.La, 05.45.−a

In recent years, propagating activity in spatially extended systems has been found experimentally in neural systems [1–5] and in chemistry and biology [6–8]. In particular traveling fronts have attracted much interest in theory [7,9–12] partly due to experimental findings [13–15]. Several studies dealing with these phenomena treat the examined system by partial differential equations, which account for short-range spatial interactions. However, neural systems might exhibit long-range interactions by their underlying spatial structure [16]. This structure originates from dendritic arborizations of neurons and from the spread of axonal connections. Hence, realistic models of neural activity have to treat nonlocal interactions by integrating kernels. These kernels reflect the underlying connectivity in neural tissue. However, connectivity kernels are known only for few functional areas as the visual cortex [17], the cerebellum [18], or the prefrontal cortex [19]. Thus, modeling of traveling phenomena in general neural systems necessitates the treatment for more general kernel types. We mention previous studies of the stability of neural fields for general homogeneous kernels [20–22]. The present work follows this idea in order to gain a classification scheme for traveling fronts. This Brief Report is similar to previous studies considering general kernels [10,11] or general synaptic responses [23], but contrasts to these studies by considering constant nonlocal feedback delay. The latter has been found experimentally in reciprocal-connected neural areas [24,25] and plays a decisive role in neural information processing [26]. We shall show how the front speed depends on both additional delays and how the typical front shape changes by the feedback delay.

The conduction-based model [27–29] assumes neural populations coupled on a microscopic spatial level by chemical synapses. That is, population ensembles represent a coarse-grained spatial field. In addition, the neural activity is expressed by dendritic currents and firing rates averaged over an ensemble entity. This assumption neglects single-spike activity and temporal coding of neurons; i.e., the neural firing times are uncorrelated [30]. Thus the model considers time-averaged spiking activity—i.e., coarse-grained temporal activity. By virtue of its mesoscopic spatial scale, such neural activity is recorded in neurophysiological experiments as local field potentials (e.g., [31]). In mathematical terms, the neural field is assumed to be continuous in space and time. The dendritic current V at location x at time t represents the linear delayed response of chemical synapses subject to incoming pulse activity. In turn, this pulse activity originates at a spatial location y by conversion from dendritic currents $V(y,t-\alpha(x,y))$. Here $\alpha(x,y)$ represents the delay time between the origin and termination of the pulse. The present work treats two types of delay (Fig. 1). One type considers pulse activity propagating along axonal connections in the field and terminating at chemical synapses. This work focuses on intracortical fields, which exhibit the same transmission speed v for both excitatory and inhibitory connections. Hence, the transmission delay is $\alpha(x,y)=|x-y|/v$. Further a nonlocal feedback loop is present with $\alpha(x,y)=\tau$, which terminates at either excitatory or inhibitory chemical synapses. We point out that both transmission and feedback delays are assumed homogeneous; i.e., the corresponding connectivity between two locations depends on their spatial distance only.

The model assumes a single time scale in the synaptic delay, which is set to unity by an appropriate time scaling. Hence, the dendritic current obeys

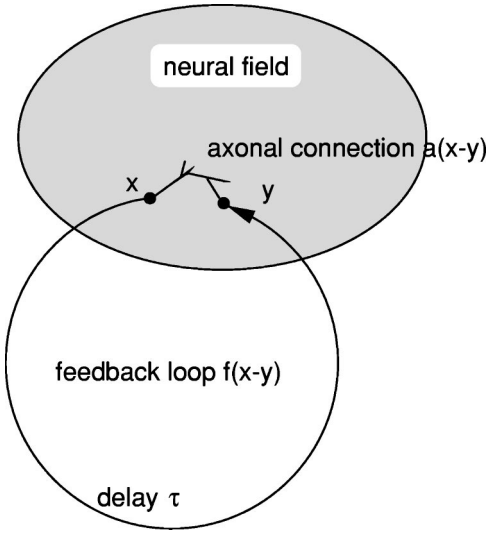

FIG. 1. Sketch of intra-areal axonal connections and nonlocal feedback connections.

*Electronic address: hutt@wias-berlin.de

$$\frac{\partial}{\partial t}V(x,t) = -V(x,t) + a(x,t) + f(x,t), \tag{1}$$

$$a(x,t) = \int_{-\infty}^{\infty} A(x-y)S(V(y,t-|x-y|/v))dy,$$

$$f(x,t) = \int_{-\infty}^{\infty} F(x-y)S(V(y,t-\tau))dy.$$

The functions $a(x,t)$ and $f(x,t)$ represent the synaptic input by axonal and feedback connections, respectively. The corresponding connectivity functions $A(x)$ and $F(x)$ are introduced as probability density functions of connections—i.e., $\int_{-\infty}^{\infty}A(x)dx=\kappa<\infty$, $\int_{-\infty}^{\infty}F(x)dx=\mu<\infty$. Here, the constants κ and μ represent the synaptic strength of axonal and nonlocal feedback contributions, respectively. The axonal transmission speed v and the constant feedback delay τ introduce two more time scales to the system, in addition to the synaptic delay. The conversion from dendritic currents to pulse rates is given by the transfer function S. It reflects the statistical properties of firing thresholds and active processes in action potential generation [28,30,32] and exhibits a sigmoidal shape. In the following, we assume the same firing thresholds V_0 for all neurons function. Thus the transfer function is chosen to the Heaviside step function $S(V)=\Theta(V-V_0)$ and the system becomes binary. A few simple calculations on Eq. (1) show the existence of two stationary constant states $V_{max}=\kappa+\mu$ and $V_{min}=0$.

Now, a transformation to the moving frame $V(x,t)=V(x-ct)=V(z)$ with the front speed c simplifies the analysis. Boundary conditions $V(z\to-\infty)=V_{max}>V_0$, $V(z\to\infty)=V_{min}<V_0$ and $V(0)=V_0$ guarantee the traveling front solutions. In addition, the condition $-v<c<v$ guarantees physically reasonable solutions consistent with previous findings [10,33,34]. Assuming $V(z)>V_0\,\forall\, z<0$ and $V(z)\leqslant V_0\,\forall\, z\geqslant 0$, Eq. (1) yields

$$-c\frac{\partial}{\partial z}V(z) + V(z) = h(z), \tag{2}$$

with

$$h(z) = \int_{-\infty}^{\delta z} A(z-z')dz' + \int_{-\infty}^{-c\tau} F(z-z')dz' \tag{3}$$

and $\delta=c/(c-v)\,\forall\, z\geqslant 0$, $\delta=c/(c+v)\,\forall\, z<0$.

Now, we examine the dependence of the front speed c from various parameters. In the case of $c>0$, solving Eq. (2) by partial integration yields divergent solutions for $z\to\infty$. However, to obtain finite solutions the sum of divergent terms g needs to vanish. Following the same path of calculations in the case of $c<0$, we find divergent solutions for $z\to-\infty$. Thus nondivergent solutions $V(z)$ stipulate $g=0$ with

$$g = \kappa/2 + \mathcal{L}[F(u+|c|\tau)](0) - V_0 \mp \mathcal{L}[A(u)] \times\left(\frac{1}{|c|}\mp\frac{1}{v}\right) \mp e^{\tau}\mathcal{L}[F(u+|c|\tau)]\left(\frac{1}{|c|}\right), \tag{4}$$

which defines the threshold V_0 subject to the parameters.

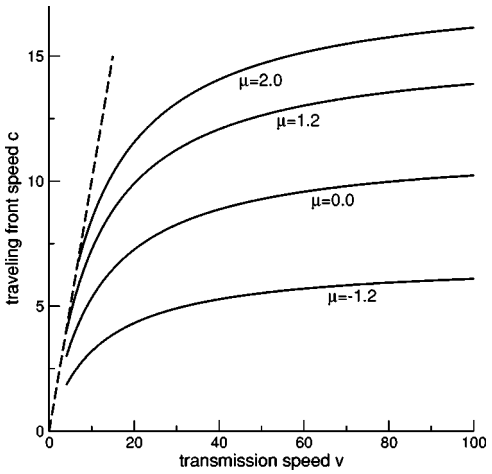

FIG. 2. The front speed plotted with respect to the transmission speed for various feedback strengths for the kernels (5). The parameters are set to $a_e=2.0$, $a_i=2.0$, $V_0=0.1$, $\tau=0.01$, $\sigma=0.8$, and $r=2.0$.

Here and in the following, $\mathcal{L}[\cdot]$ denotes the Laplace transform and the upper (lower) sign represents the case $c\geqslant 0$ ($c<0$). As shall be seen in the subsequent paragraph, Eq. (4) defines the resulting front speed for fixed threshold V_0.

In a first analysis step, we neglect the feedback $F=0$. Utilizing the relations $(\partial g/\partial v)\,dv=-g'\,dc$ and $g'=\partial g/\partial c$, we find the relation $dc/dv=-(\partial g/\partial v)/g'$. It turns out that $\partial g/\partial v=\mathcal{L}[uA(u)](w)/v^2$ and $g'=-\mathcal{L}[uA(u)](w)/c^2$ with $w=1/|c|\mp 1/v$. This leads to $dc/dv=c^2/v^2$ for all kernels A. That is, the front speed monotonically increases with increasing transmission speed for all axonal kernels. Additionally, for $v\to\infty$, the front speed c saturates to c_0 with $V_0-\kappa/2=\mp\mathcal{L}[A](1/|c_0|)$.

In order to study the case $F\neq 0$ in some detail, the analysis focuses on the family of exponential kernels,

$$A(z) = \frac{a_e}{2}e^{-|z|} - \frac{a_i r}{2}e^{-r|z|}, \quad F(z) = \frac{\mu}{2\sigma}e^{-|z|/\sigma}, \tag{5}$$

where σ gives the spatial feedback range, a_e and a_i are excitatory and inhibitory weights, and r abbreviates the ratio of excitatory and inhibitory spatial ranges (cf. [34]). For instance, in the case of $a_e=a_i$, $r<1$ and $r>1$ correspond to local excitation-lateral inhibition and local inhibition-lateral excitation, respectively. With these definitions Eq. (4) is recast into

$$g = \frac{a_e}{2}\frac{v-|c|}{v-|c|+v|c|} - \frac{a_i}{2}\frac{v-|c|}{v-|c|+rv|c|} + \frac{\mu}{2}\frac{\sigma}{\sigma+|c|}e^{-|c|\tau/\sigma} - V_0. \tag{6}$$

We find $dc/dv=c^2/(v^2+b\mu)$ with $b=b(|c|,v,\sigma,\tau,a_e,a_i)$. Figure 2 shows the relation of c and v for excitatory and inhibitory feedback, which is similar to results in previous studies for vanishing feedback loops (cf. [10,23]). Further, the figure indicates a monotonic increase (decrease) of the front speed by increased excitatory (inhibitory) feedback. In

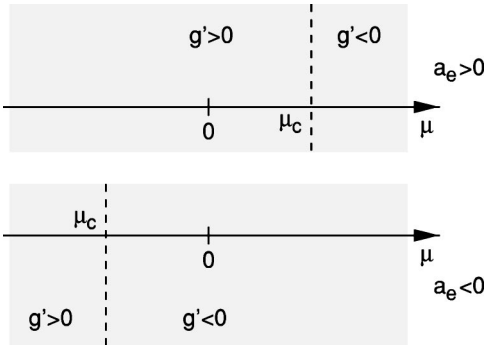

FIG. 3. Sketch of the relation between μ and g'.

order to examine this relation in some more detail, we focus on $dc/d\mu=-(\partial g/\partial\mu)/g'$. First let us take a look at the sign of g'. We find, for $a_i=0$ and $v\gg|c|$,

$$\mu_c = a_e\left[\frac{1+|c|}{\sigma+|c|}\left(\tau+\frac{\sigma}{\sigma+|c|}\right)e^{-|c|\tau/\sigma}\right]^{-1}$$

for $g'=0$. It turns out that excitatory fields with $a_e>0$ yield $\mu_c>0$ and Eq. (6) gives $\partial g/\partial\mu\geqslant 0$ for $\mu\geqslant 0$. In addition, it is $g'<0$ for $\mu>\mu_c$ which leads to $dc/d\mu>0$ for $\mu>\mu_c$. That is, increasing excitatory feedback in excitatory fields increases the front speed. In the case of $0<\mu<\mu_c$, it is $g'>0$ and $dc/d\mu<0$; i.e., increasing excitatory feedback may also reveal decreasing front speeds. Figure 3 summarizes the results and confirms Fig. 2. Inhibitory fields with $a_e<0$ yield $\mu_c<0$ and the resulting relations can be derived in a similar way by Fig. 3. With these results, it is straightforward to find the relation of the front speed to the feedback delay and the feedback range. It is $dc/d\tau=\mu a/g'$ and $dc/d\sigma=-\mu b/g'$ with $a(c,\sigma,\tau)>0$ and $b(c,\sigma,\tau)>0$. Figure 4 illustrates these relations for parameters with $g'<0$. Interestingly, it is also $d\sigma/d\tau=a/b>0$ for constant c. That is, increased feedback delay times demand an increased feedback range for constant front speeds. The level lines in Fig. 4 confirms this result.

Finally, we focus on the shape of the traveling front and find, for general kernels,

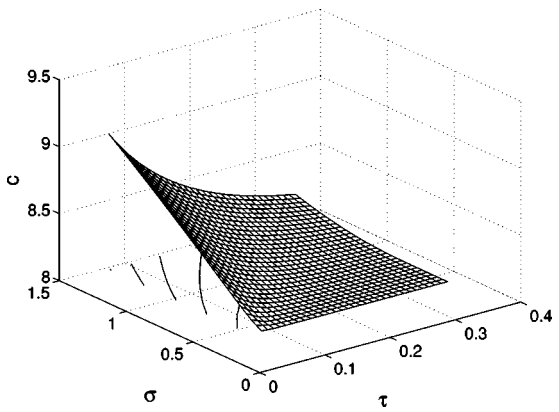

FIG. 4. The front speed c with respect to the feedback range σ and the feedback delay τ for the kernels (5). Other parameters are $a_e=2.0$, $a_i=0.0$, $V_0=0.1$, and $\mu=7.81$.

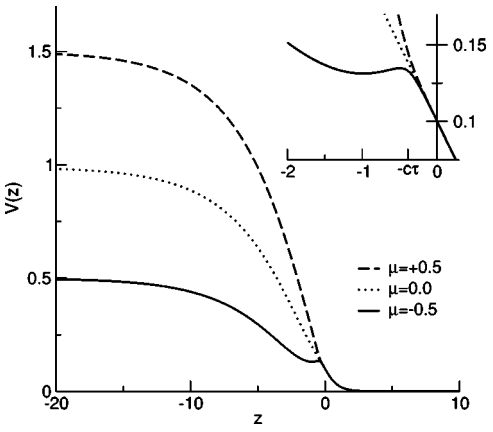

FIG. 5. The traveling front for excitatory, vanishing, and inhibitory nonlinear feedback for the kernels (5). Parameters are $a_e=2.0$, $a_i=1.0$, $r=2.0$, $V_0=0.1$, $\tau=0.1$, $\sigma=0.1$, $v=10.28$, and $c\approx 3.9$ for all applied values of μ.

$$\begin{aligned}V(z) &= \int_{-\infty}^{\delta z} A(z-u)du + \int_{-\infty}^{-c\tau} F(z-u)du \\ &+ \int_0^z [(1-\delta)A((1-\delta)u) + F(u+c\tau)]e^{(z-u)/c}du \\ &\mp e^{z/c}\left[\mathcal{L}[A(u)]\left(\frac{1}{|c|}\mp\frac{1}{v}\right) + e^{\tau}\mathcal{L}[F(u+|c|\tau)]\left(\frac{1}{|c|}\right)\right].\end{aligned} \tag{7}$$

Typical traveling fronts exhibit a single inflection point and approach horizontal asymptotics for $|z|\to\infty$. However, a close look at Eq. (2) indicates a sign change of dV/dz due to nonlocal feedback; i.e., local extrema of $V(z)$ may exist. Considering Eqs. (2) and (7) the sufficient condition for local extrema reads

$$\begin{aligned}&\mathcal{L}[A(u)]\left(\frac{1}{|c|}\mp\frac{1}{v}\right) + e^{\tau}\mathcal{L}[F(u+|c|\tau)]\left(\frac{1}{|c|}\right) \\ &= \pm\int_0^{z_e}[(1-\delta)A((1-\delta)u) + F(u+|c|\tau)]e^{-u/c}du.\end{aligned} \tag{8}$$

That is, the typical shape of the traveling front is changed if Eq. (8) shows real roots z_e. In addition, the type of extrema is given by the sign of

$$\left.\frac{\partial^2 V}{\partial z^2}\right|_{z=z_e} = \frac{(1-\delta)}{c}A(z_e(1-\delta)) + \frac{1}{c}F(z_e+c\tau). \tag{9}$$

Now recall the implicit condition $\partial V/\partial z<0$ at $z=0$. This condition constrains the set of possible local extrema. For $z_e>0$, Eq. (8) needs an even number of solutions with both positive and negative signs of $\partial^2 V/\partial z^2$ at $z=z_e$. In contrast, $z_e<0$ facilitates an arbitrary number of extrema with at least one maximum. Figure 5 shows the novel shape by plotting $V(z)$ from Eq. (7) for appropriate parameters. Here, inhibitory feedback results in a local minimum and maximum,

while excitatory feedback does show the typical shape with a steeper front. Assessing these analytical solutions numerically by inserting them to Eq. (2) reveals good accordance (not shown).

A further sufficient criterion for the occurrence of local extrema is the existence of a horizontal inflection point, from which both a local minimum and local maximum grow by changing parameters. According to Eq. (9), the corresponding condition reads

$$\frac{v}{v+c}A\left(\frac{vz}{v+c}\right) = -F(z+c\tau). \tag{10}$$

It turns out that excitatory fields—i.e., $A>0$—exhibit local extrema only in the case of inhibitory feedback with $F<0$, while $A<0$ faciliates extrema for $F>0$ only. In other words no local extrema occur in excitatory (inhibitory) fields subject to excitatory (inhibitory) feedback.

The previous sections showed the existence of traveling fronts, while no information is gained about their temporal stability towards small deviations. This problem has been attacked recently by considering Evans functions of nonlocal neural fields [35,36]. Though this stability analysis of the proposed model might yield novel interesting results, it would exceed the major aim of this Brief Report and we refer the reader to future work.

Summarizing, the present Brief Report introduces nonlinear feedback to neural fields and investigates its influence on the speed of traveling fronts and its shape for general connectivity kernels. The novel front shape emerges due to nonlocal feedback of contrary sign of interaction with the field—i.e., in the case of excitatory feedback in inhibitory fields and vice versa.

This work was supported by the DFG research center "Mathematics for key techonologies" (FZT 86) in Berlin, Germany.

[1] U. Kim, T. Bal, and D. McCormick, J. Neurophysiol. **74**, 1301 (1995).
[2] D. Golomb and Y. Amitai, J. Neurophysiol. **78**, 1199 (1997).
[3] A. Arieli, D. Shoham, R. Hildesheim, and A. Grinvald, J. Neurophysiol. **73**, 2072 (1995).
[4] H. Spors and A. Grindvald, Neuron **34**, 301 (2002).
[5] J. Y. Wu, L. Guan, and Y. Tsau, J. Neurosci. **19**, 5005 (1999).
[6] J. Murray, *Mathematical Biology* (Springer, Berlin, 1989).
[7] E. Meron, Phys. Rep. **218**, 1 (1992).
[8] Y. Kuramoto, *Chemical Oscillations, Waves, and Turbulence* (Springer, Berlin, 1984).
[9] R. Osan and G. B. Ermentrout, Physica D **163**, 217 (2002).
[10] D. J. Pinto and G. B. Ermentrout, SIAM (Soc. Ind. Appl. Math.) J. Appl. Math. **62**, 206 (2001).
[11] Z. Chen, B. Ermentrout, and B. McLeod, Appl. Anal. **3-4**, 235 (1997).
[12] D. Panja, Phys. Rep. **393**, 87 (2004).
[13] W. van Saarloos, M. van Hecke, and R. Holyst, Phys. Rev. E **52**, 1773 (1995).
[14] S. J. DiBartolo and A. T. Dorsey, Phys. Rev. Lett. **77**, 4442 (1996).
[15] J. Fineberg and V. Steinberg, Phys. Rev. Lett. **58**, 1332 (1987).
[16] M. Abeles, *Corticonics* (Cambridge University Press, Cambridge, England, 1991).
[17] S. LeVay and S. Nelson, in *The Neural Basis of Visual Function*, edited by J. Cronly-Dillon (Macmillan, London, 1991), pp. 266–315.
[18] C. Saab and W. Willis, Brain Res. Rev. **42**, 85 (2003).
[19] J. Levitt, D. Lewis, T. Yishioka, and J. Lund, J. Comp. Neurol. **338**, 360 (1993).
[20] S. Amari, Biol. Cybern. **27**, 77 (1977).
[21] B. Ermentrout, J. McLeod, and J. Bryce, Proc. - R. Soc. Edinburgh, Sect. A: Math. **123**, 461 (1993).
[22] F. M. Atay and A. Hutt, SIAM (Soc. Ind. Appl. Math.) J. Appl. Math. (to be published).
[23] S. Coombes, G. J. Lord, and M. R. Owen, Physica D **178**, 219 (2003).
[24] M. Steriade, E. G. Jones, and R. R. Llinas, *Thalamic Oscillations and Signaling* (Wiley, New York, 1990).
[25] C. Cavada and P. S. Goldman-Rakic, Prog. Brain Res. **95**, 123 (1993).
[26] W. Singer, Neuron **24**, 49 (1999).
[27] H. R. Wilson and J. D. Cowan, Biophys. J. **12**, 1 (1972).
[28] B. Ermentrout, Neural Comput. **6**, 679 (1994).
[29] V. K. Jirsa and H. Haken, Phys. Rev. Lett. **77**, 960 (1996).
[30] W. Gerstner, Phys. Rev. E **51**, 738 (1995).
[31] A. Destexhe, D. Contreras, and M. Steriade, J. Neurosci. **19**, 4595 (1999).
[32] D. J. Amit, *Modeling Brain Function: The World of Attractor Neural Networks* (Cambridge University Press, Cambridge, England, 1989).
[33] V. Bringuier, F. Chavane, L. Glaeser, and Y. Fregnac, Science **283**, 695 (1999).
[34] A. Hutt, M. Bestehorn, and T. Wennekers, Network Comput. Neural Syst. **14**, 351 (2003).
[35] L. Zhang, Diff. Integral Eq. **16**, 513 (2003).
[36] S. Coombes and M. R. Owen, SIAM J. Appl.. Dyn. Syst. (to be published).